

Fungus-Mediated Synthesis of Silver Nanoparticles and Their Immobilization in the Mycelial Matrix: A Novel Biological Approach to Nanoparticle Synthesis

Priyabrata Mukherjee,[†] Absar Ahmad,[‡] Deendayal Mandal,[†] Satyajyoti Senapati,[†] Sudhakar R. Sainkar,[§] Mohammad I. Khan,[‡] Renu Parishcha,[§] P. V. Ajaykumar,^{||} Mansoor Alam,^{||} Rajiv Kumar,^{*,†} and Murali Sastry^{*,§}

*Divisions of Catalysis, Biochemical Science, and Materials Chemistry,
National Chemical Laboratory, Pune - 411 008, India*

Received March 14, 2001; Revised Manuscript Received August 10, 2001

ABSTRACT

A novel biological method for the synthesis of silver nanoparticles using the fungus *Verticillium* is reported. Exposure of the fungal biomass to aqueous Ag⁺ ions resulted in the intracellular reduction of the metal ions and formation of silver nanoparticles of dimensions 25 ± 12 nm. Electron microscopy analysis of thin sections of the fungal cells indicated that the silver particles were formed below the cell wall surface, possibly due to reduction of the metal ions by enzymes present in the cell wall membrane. The metal ions were not toxic to the fungal cells and the cells continued to multiply after biosynthesis of the silver nanoparticles.

Introduction. The field of nanotechnology has witnessed impressive advances in various aspects such as the synthesis of nanoscale matter and understanding/utilizing their exotic physicochemical and optoelectronic properties. Recent developments in our understanding of self-assembly processes has led to newer approaches for the organization of nanoparticles into predefined superstructures, thus ensuring that nanotechnology will play an increasingly important role in many key technologies of the new millennium.¹ Commercial application of nanoparticles requires their assembly and packaging in thin film form, and toward this end the “bottom-up” approach has been receiving considerable attention.^{2,3} There is a growing need to develop clean, nontoxic and environmentally friendly (“green chemistry”) procedures for synthesis and assembly of nanoparticles, which has resulted in researchers seriously looking at biological systems for inspiration. This (together with purely academic curiosity) has led to the development of biomimetic approaches for the growth of advanced materials. There is no dearth of

examples in both the plant and animal kingdom of unicellular and multicellular organisms that produce inorganic materials either intra- or extracellularly.⁴ Some of the more well-known examples include magnetotactic bacteria (which synthesize magnetite nanoparticles),⁵ diatoms (which synthesize siliceous materials),⁶ and S-layer bacteria (which produce gypsum and calcium carbonate layers).⁷

Although biotechnological applications such as remediation of toxic metals use microorganisms such as bacteria and yeasts extensively⁸ (the detoxification often occurring by formation of metal sulfides),⁹ reports on the use of such microorganisms to synthesize advanced materials and, in particular, nanoscale materials have been at best sporadic.^{10–12} In focusing on the biosynthesis of nanomaterials, Klaus-Joerger and co-workers have demonstrated that the bacterium *Pseudomonas stutzeri* AG259 isolated from a silver mine, when placed in a concentrated aqueous solution of AgNO₃, was able to reduce the Ag⁺ ions and form silver nanoparticles of well-defined size and distinct morphology within the periplasmic space of the bacteria.¹¹ Taking this approach a step further, they have shown that biocomposites of nanocrystalline silver and the bacteria may be thermally treated to yield a carbonaceous material with interesting optical properties for potential application in functional thin film coatings.¹² The exact reaction mechanism leading to the

* Corresponding authors. E-mail: rajiv@cata.ncl.res.in; sastry@ems.ncl.res.in

[†] Catalysis division.

[‡] Biochemical Science division.

[§] Materials Chemistry division.

^{||} Current address: Department of Microbiology and Plant Pathology, Central Institute of Medicinal and Aromatic Plants, P. O. CIMAP, Lucknow 226 015, India.

formation of silver nanoparticles by this species of silver-resistant bacteria is yet to be elucidated. Beveridge and co-workers also have used bacteria for the intracellular synthesis of gold nanoparticles by the reduction of aqueous Au^{3+} ions.¹³ Developing on the strategy to enlarge the scope of bioorganisms in the synthesis of nanomaterials, we demonstrate herein that the fungus *Verticillium* (AAT-TS-4), when exposed to aqueous AgNO_3 solution, causes the reduction of the metal ions and formation of silver nanoparticles of ca. 25 nm diameter. The silver nanoparticles are formed below the surface of the fungal cells with negligible reduction of the metal ions observed in solution. It is to be noted that, in contrast to the earlier studies on the use of yeast cells in the synthesis of metal sulfides,^{9,10} metallic silver nanoparticles are obtained with the fungus *Verticillium*, thus pointing to a radically different mechanism for the reduction of the Ag^+ ions present in solution. Presented below are details of the investigation.

Experimental Details. The fungus *Verticillium* was isolated from the *Taxus* plant and maintained on potato-dextrose agar slants at 25 °C. The fungus was grown in 500 mL Erlenmeyer flasks, each containing 100 mL MGYB media composed of malt extract (0.3%), glucose (1.0%), yeast extract (0.3%), and peptone (0.5%) at 25–28 °C under shaking conditions (200 rpm) for 96 h. After 96 h of fermentation, mycelia were separated from the culture broth by centrifugation (5000 rpm) at 10 °C for 20 min, and the settled mycelia was washed thrice with sterile distilled water. Ten grams of the harvested mycelial mass was then resuspended in 100 mL sterile distilled water in 500 mL conical flasks at pH = 5.5–6.0. To this suspension, 100 mL of an aqueous solution of 2×10^{-4} M AgNO_3 was added, thus leading to an overall concentration of Ag^+ ions in the reaction mixture of 10^{-4} M. The whole mixture was thereafter put into a shaker at 28 °C (200 rpm) and the reaction carried out for a period of 72 h. The biotransformation was routinely monitored by visual inspection of the biomass as well as measurement of the UV–vis spectra from the fungal cells and the aqueous medium in the reaction mixture. After this reaction period, the biomass was washed thrice with copious amounts of sterile distilled water prior to preparation of the biofilms for analysis. Films of the fungal cells (both before and after exposure to Ag^+ ions for 72 h) for UV–vis spectroscopy, X-ray diffraction (XRD), and scanning electron microscopy (SEM) studies were prepared by solution-casting the washed fungal cells onto Si(111) wafers and thoroughly drying the film in flowing N_2 . UV–vis spectroscopy measurements of the films were made on a Shimadzu dual-beam spectrophotometer (model UV-1601PC) operating in the reflection mode at a resolution of 2 nm. Since the films of the bionanocomposite were rough, the results are not quantitative and have been used to merely detect the presence of silver nanoparticles in the biomaterial. UV–vis spectra of the aqueous AgNO_3 solution as a function of time of reaction as well as after 72 h of reaction with the mycelial cells were also carried out in the transmission mode on the same instrument. Scanning electron microscopy (SEM) and energy dispersive analyses of X-ray (EDX)

measurements of the fungal cells after formation of silver nanoparticles were carried out on a Leica Stereoscan-440 SEM equipped with a Phoenix EDX attachment. EDX spectra were recorded in the spot-profile mode by focusing the electron beam onto a region on the surface of the mycelial cells rich in silver nanoparticles.

To investigate the exact location of the silver nanoparticles in relation to the *Verticillium* cells, transmission electron microscopy (TEM) studies of thin sections of the Ag nano-*Verticillium* cells were carried out. The procedure for preparation and staining of the thin sections of the Ag nano-*Verticillium* cells was identical to that used by Klaus et al. in their study of silver-resistant bacteria^{11a} and for brevity, will not be repeated here. TEM analysis of thin sections of the biofilms placed on 40 μm mesh copper grids was carried out on a JEOL Model 1200EX instrument operated at an accelerating voltage of 60 kV. A low operating voltage was used to minimize damage to the thin sections by electron beam heating.

Results and Discussion. Figure 1A shows a conical flask of the fungal cells after removal from the culture medium and before immersion in AgNO_3 solution. The pale yellow color of the fungal cells can clearly be seen in the figure. A picture of the conical flask containing the fungal cells after exposure to 10^{-4} M aqueous solution of AgNO_3 for 72 h is shown in Figure 1B. A dark brown color is clearly seen in the fungal cells and indicates the synthesis of Ag nanoparticles by the cells. It is to be noted that Figure 1B shows the fungal cells along with the AgNO_3 solution. It is clear that the aqueous medium is colorless, thereby strongly indicating that extracellular reduction of Ag^+ ions had not occurred. It is well-known that silver nanoparticles absorb radiation in the visible region of the electromagnetic spectrum (ca. 380–450 nm) due to excitation of surface plasmon vibrations, and this is responsible for the striking yellow-brown color of silver nanoparticles in various media.¹⁴ Figure 1C shows the UV–vis spectra recorded from a film of the fungal cells before (curve 1) and after immersion in 10^{-4} M AgNO_3 solution for 72 h (curve 5). While there is no evidence of absorption in the spectral window 400–800 nm in the case of the as-harvested fungal cells, the fungal cells exposed to Ag^+ ions show a distinct and fairly broad absorption band centered at ca. 450 nm. The presence of the broad resonance indicates an aggregated structure of the silver particles in the film. As mentioned earlier, scattering from the rough biomass surface would also contribute to the broadening of the resonance. The wavelength of the resonance is close to that observed for thin films of silver nanoparticles complexed with fatty lipid lamellae in Langmuir–Blodgett films^{14c} as well as in thermally evaporated lipid matrices.^{14d} It is important to note that the UV–vis spectrum recorded from the fungal cells after immersion in AgNO_3 solution (Figure 1C, curve 5) is characteristic of aggregated silver nanoparticles and *not silver sulfide nanoparticles*.¹⁵ This thus rules out the role of peptides such as glutathione, which have been implicated in the formation of metal sulfide nanoparticles such as CdS^{10b} and Ag_2S^{15} by reacting yeast cells with the appropriate metal ions. The mechanism for the formation of

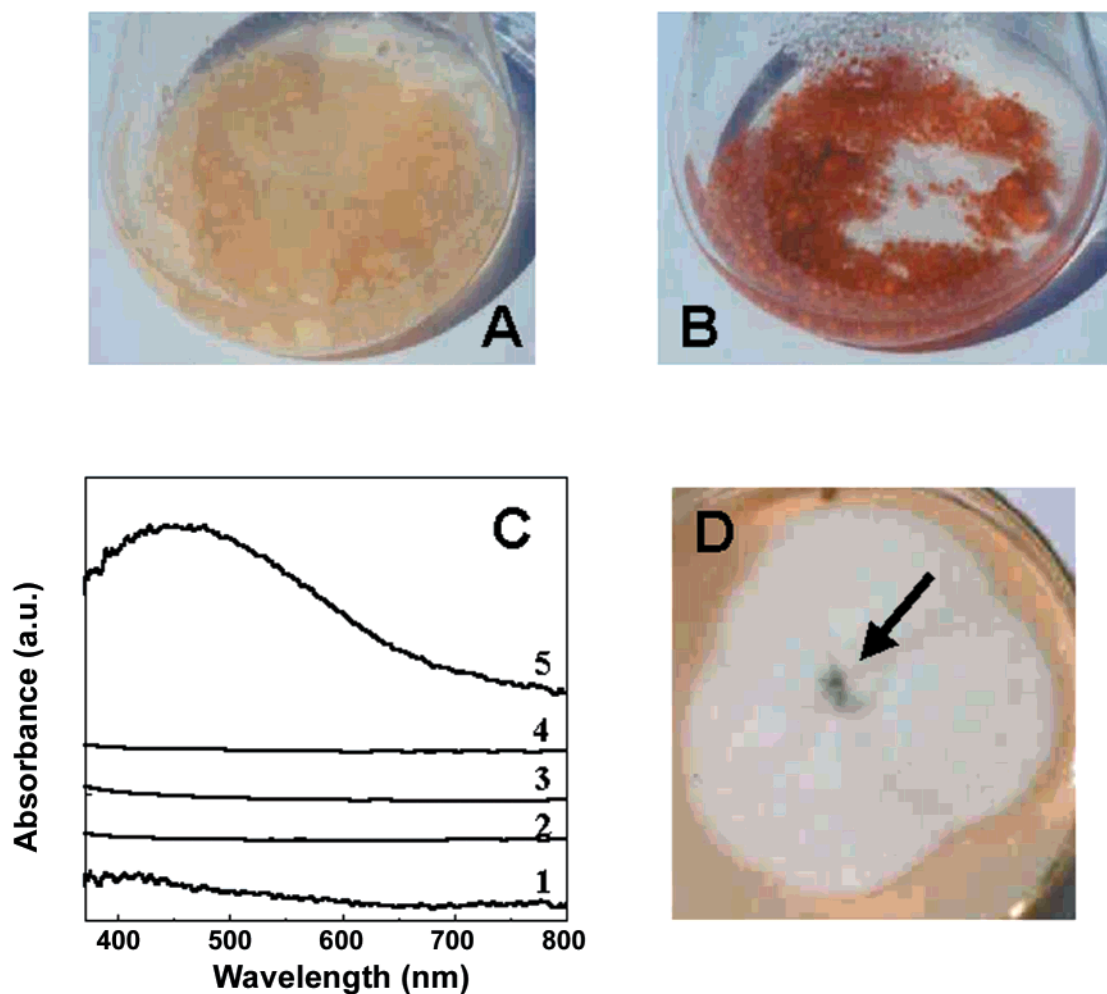


Figure 1. Conical flasks showing the *Verticillium* biomass before (A) and after immersion in 10^{-4} M aqueous AgNO_3 solution for 72 h (B). The biomass in Figure 1B is shown along with the AgNO_3 solution on completion of the 72 h reaction time. (C) UV-vis spectra recorded from films of the fungal cells before (curve 1) and after immersion in 10^{-4} M aqueous AgNO_3 solution for 72 h (curve 5). Curves 2–4 correspond to spectra recorded from the AgNO_3 phase after 6, 24, and 48 h of exposure to the biomass, respectively. (D) Picture showing the growth of the *Verticillium* after reaction with Ag^+ ions for 72 h. The dark core (indicated by arrows) is the seed Ag nano-*Verticillium* biofilm which grew to cover the surface of the agar plate (whitish mass) within one week.

silver nanoparticles by the fungus *Verticillium* is thus radically different and is an important result of this investigation.

A possible mechanism for the presence of silver nanoparticles in the fungal biomass could be the extracellular reduction of the Ag^+ ions in solution followed by precipitation onto the cells. UV-vis spectra recorded from the aqueous AgNO_3 solution after 6, 24, and 48 h of reaction with the biomass are shown as curves 2, 3, and 4, respectively, in Figure 1C. The curves have been displaced vertically for clarity. It is clear that there is negligible presence of silver particles in solution, thus clearly pointing to intracellular/surface reduction of the Ag^+ ions as the most probable mechanism for the synthesis of the silver nanoparticles by the fungus.

Figure 2A shows an SEM picture of the fungal cells after exposure to 10^{-4} M aqueous AgNO_3 solution for 72 h. The highly filamentary nature of the mycelia is clearly seen in the figure. The presence of uniformly distributed silver nanoparticles on the surface of the fungal cells is observed, indicating that the nanoparticles formed by the reduction of

Ag^+ ions are bound to the surface of the cells. The silver nanoparticles seen outside the mycelia may be due to weakly bound silver nanoparticles dislodged from the biomass during preparation of the films for SEM investigation which, it may be recollected, involves washing the biomass thrice with distilled water. It is also possible that the cell walls of a small fraction of the mycelia rupture during the wash treatment due to osmotic pressure. However, that this is indeed a small percentage is shown by the fact that the Ag nano-*Verticillium* cells are alive after the Ag^+ ion treatment and wash cycles (Figure 1D). The picture in Figure 1D shows a small amount of the Ag nano-*Verticillium* biomass (dark core identified by an arrow) placed on an agar plate in the culture medium for one week. It is observed that the cells multiply (white mass) and almost completely cover the agar plate (8 cm diameter) in one week. The *Verticillium* clearly does not die either on exposure to Ag^+ ions or after washing prior to measurement. Thus, the full capability of using microorganisms in the synthesis of nanoscale materials may be realized if their ability to multiply (and cover large surface areas) is

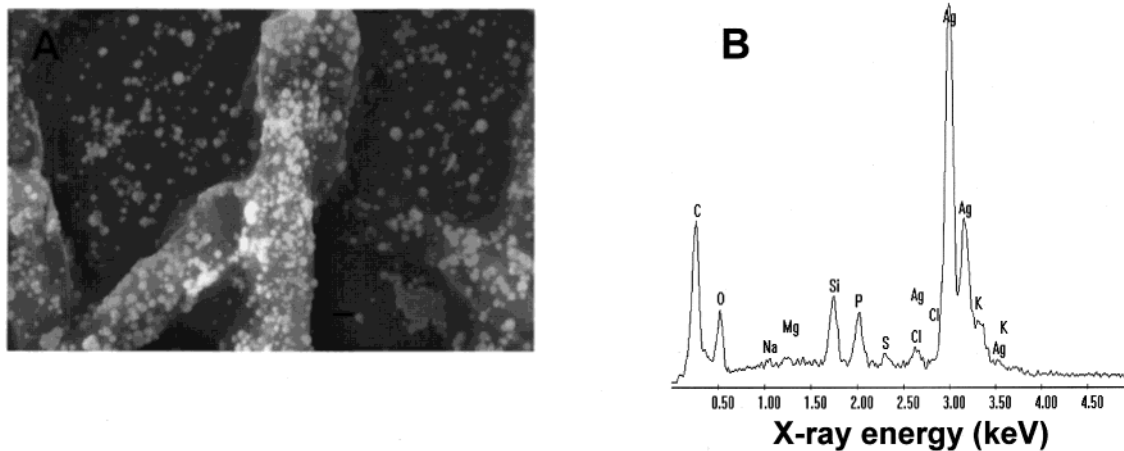


Figure 2. (A) SEM image of the *Verticillium* fungal cells after immersion in 10^{-4} M aqueous AgNO_3 solution for 72 h (scale bar = $1\ \mu\text{m}$). (B) EDX spectrum recorded from a film of the fungal cells after formation of silver nanoparticles. The different X-ray emission peaks are labeled in the figure.

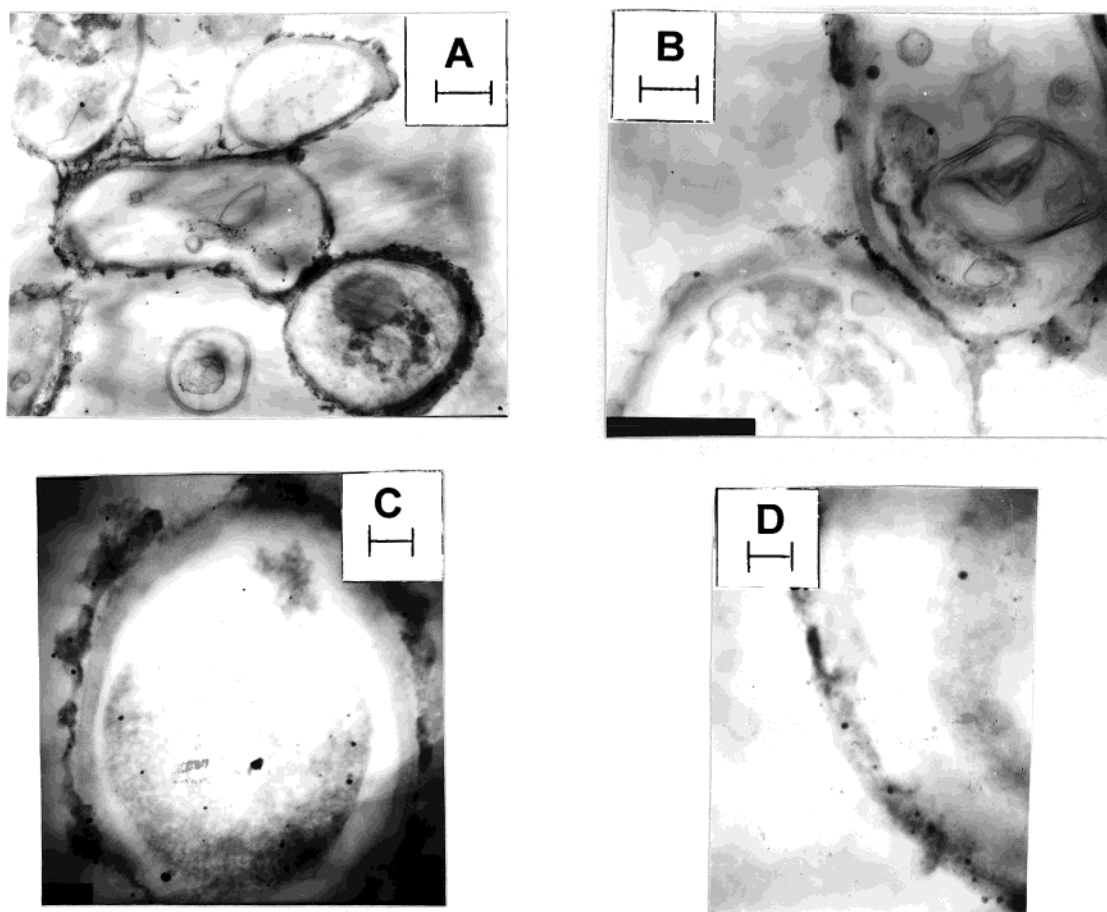


Figure 3. TEM images of thin sections of stained *Verticillium* cells after reaction with Ag^+ ions for 72 h at different magnifications (A–D). The scale bars in A–D correspond to $1\ \mu\text{m}$, 500, 200, and 100 nm respectively.

not compromised on exposure to metal ions as demonstrated in this work.

Figure 2B shows the EDX spectrum recorded in the spot-profile mode from one of the densely populated silver nanoparticle regions on the surface of the fungal cells. Strong signals from the silver atoms in the nanoparticles are observed, while weaker signals from C, O, S, P, Mg, and Na atoms were also recorded. The C, O, S, P, Mg, and Na

signals are likely to be due to X-ray emission from proteins/enzymes present in the cell wall of the biomass.

Information on the location of the silver nanoparticles relative to the fungal cells would be important in elucidating the mechanism of their formation and may be obtained by TEM analysis of thin sections of the Ag nano-*Verticillium* cells. Figure 3 shows representative TEM images at various magnifications of the *Verticillium* cells. At lower magnifica-

tion, a number of mycelia can be observed, which on closer examination reveal assemblies of *Verticillium* cells within the mycelia (Figure 3A). This image shows small particles of silver organized on the mycelial walls as cells as well as some larger particles within the cells. Figure 3B shows a slightly higher magnification image of the junction between two mycelia wherein the individual cells are more clearly resolved. A number of silver particles can be seen on the mycelia wall surface. The mycelia in the upper right corner also shows an individual *Verticillium* cell with silver particles clearly bound to the surface of the cytoplasmic membrane. Figure 3C shows a single *Verticillium* cell with silver nanoparticles both on the cell wall (external boundary) and on the cytoplasmic membrane (inner boundary). Occasionally, large silver particles could be observed within the cytoplasm of the *Verticillium* cells (Figure 3C). Selected area diffraction analysis of a single silver particle (data not shown) revealed diffuse rings with lattice spacings, in excellent agreement with those expected for silver. Analysis of the size of the silver nanoparticles from many different TEM images of the Ag nano-*Verticillium* cells yielded a particle diameter of 25 ± 12 nm. Please note that in the analysis of the silver particle sizes, the larger particles observed in the cell cytoplasm were excluded.

Figure 3D shows a higher magnification TEM image of the cell wall of one of the *Verticillium* cells after Ag nanoparticle formation. A number of silver particles are observed that are essentially spherical in morphology with fairly good monodispersity. In this respect, our results differ from those of Klaus et al. who observed that silver nanoparticles formed within the periplasmic space of silver resistant bacteria showed morphologies ranging from spherical to triangular to hexagonal.¹¹

While the exact mechanism leading to the formation of silver nanoparticles by reaction with the fungal cells is not understood at the moment, based on the results presented above, we speculate the following. Since the nanoparticles are formed on the surface of the mycelia and not in solution, we believe that the first step involves trapping of the Ag^+ ions on the surface of the fungal cells. This may occur via electrostatic interaction between the Ag^+ and negatively charged carboxylate groups in enzymes present in the cell wall of the mycelia. Thereafter, the silver ions are reduced by enzymes present in the cell wall leading to the formation of silver nuclei, which subsequently grow by further reduction of Ag^+ ions and accumulation on these nuclei. The TEM results indicate the presence of some silver nanoparticles on the cytoplasmic membrane as well as within the cytoplasm (Figure 3). It is possible that some Ag^+ ions diffuse through the cell wall and are reduced by enzymes present on the cytoplasmic membrane and within the cytoplasm. It may also be possible that some of the smaller silver nanoparticles diffuse across the cell wall to be trapped within the cytoplasm. We are currently attempting a more detailed

structural study of the Ag nano-*Verticillium* cells to understand the mechanism of silver nanoparticle formation better.

In conclusion, the bioreduction of aqueous Ag^+ ions by the fungus *Verticillium* has been demonstrated. The reduction of the metal ions occurs on the surface of the mycelia leading to the formation of silver nanoparticles of fairly well-defined dimensions and tolerable monodispersity. This fungal-mediated green chemistry approach toward the synthesis of silver nanoparticles has many advantages such as ease with which the process can be scaled up, economic viability, possibility of easily covering large surface areas by suitable growth of the mycelia, etc. The shift from bacteria to fungi as a means of developing natural "nanofactories" has the added advantage that downstream processing and handling of the biomass would be much simpler. Further, compared to bacteria, fungi are known to secrete much higher amounts of proteins, thereby significantly increasing the productivity of this biosynthetic approach. Applications of such bionanocomposites in catalysis and other electronic applications are currently being pursued.

References

- (1) Edelstein, A. S.; Cammarata, R. C., Eds.; *Nanomaterials: synthesis, properties and applications*; IOP Publishing: Bristol, U.K.; 1996.
- (2) Philip, D.; Stoddart, J. F. *Angew. Chem., Int. Ed.* **1996**, *35*, 1155.
- (3) (a) Fendler, J. H.; Meldrum, F. C. *Adv. Mater.* **1995**, *5*, 607. (b) Sastry, M. *Curr. Sci.* **2000**, *78*, 1089. (c) Shipway, A. N.; Katz, E.; Willner, I. *ChemPhysChem.* **2000**, *1*, 19.
- (4) (a) Simkiss, K.; Wilbur, K. M. *Biomining*; Academic Press: New York, 1989. (b) Mann, S., Ed.; *Biomimetic Materials Chemistry*; VCH: Weinheim, 1996.
- (5) (a) Spring, H.; Schleifer, K. H. *System. Appl. Microbiol.* **1995**, *18*, 147. (b) Dickson, D. P. E. *J. Magn. Magn. Mater.* **1999**, *203*, 46.
- (6) (a) Mann, S. *Nature* **1993**, *365*, 499. (b) Oliver, S.; Kupermann, A.; Coombs, N.; Lough, A.; Ozin, G. A. *Nature* **1995**, *378*, 47.
- (7) (a) Pum, D.; Sleytr, U. B. *Trends Biotechnol.* **1999**, *17*, 8. (b) Sleytr, U. B.; Messner, P.; Pum, D.; Sara, M. *Angew. Chem., Int. Ed. Engl.* **1999**, *38*, 1034.
- (8) (a) Duncan, J. R.; Brady, D.; Wilhelmi, B. *Methods Biotech.* **1997**, *2*, 91. (b) Stephen, J. R.; Maenoughton, S. J. *Curr. Opin. Biotechnol.* **1999**, *10*, 230.
- (9) Mehra, M. K.; Winge, D. R. *J. Cell. Biochem.* **1991**, *45*, 30.
- (10) (a) Mehra, R. K.; Tarbet, E. B.; Gray, W. R.; Winge, D. R. *Proc. Natl. Acad. Sci. U.S.A.* **1988**, *85*, 8815. (b) Dameron, C. T.; Reese, R. N.; Mehra, R. K.; Kortan, P. J.; Carrol, M. L.; Steigerwald, M. L.; Brus, L. E.; Winge, D. R. *Nature* **1989**, *338*, 596.
- (11) (a) Klaus, T.; Joerger, R.; Olsson, E.; Granqvist, C.-G. *Proc. Natl. Acad. Sci. U.S.A.* **1999**, *96*, 13611. (b) Klaus-Joerger, T.; Joerger, R.; Olsson, E.; Granqvist, C.-G. *Trends Biotech.* **2001**, *19*, 15.
- (12) Joerger, R.; Klaus, T.; Granqvist, C.-G. *Adv. Mater.* **2000**, *12*, 407.
- (13) (a) Beveridge, T. J.; Murray, R. G. E. *J. Bacteriol.* **1980**, *141*, 876. (b) Southam, G.; Beveridge, T. J. *Geochim. Cosmochim. Acta* **1996**, *60*, 4369. (c) Fortin, D.; Beveridge, T. J. In *Biomining: From Biology to Biotechnology and Medical Applications*; Baeuerlein, E., Ed.; Wiley-VCH: Weinheim, 2000; p 7.
- (14) (a) Henglein, A. *J. Phys. Chem.* **1993**, *97*, 5467. (b) Sastry, M.; Bandyopadhyay, K.; Mayya, K. S. *Coll. Surf. A* **1997**, *127*, 221. (c) Sastry, M.; Mayya, K. S.; Patil, V.; Paranjape, D. V.; Hegde, S. G. *J. Phys. Chem. B* **1997**, *101*, 4954. (d) Sastry, M.; Patil, V.; Sainkar, S. R. *J. Phys. Chem. B* **1998**, *102*, 1404.
- (15) Brelle, M. C.; Zhang, J. Z.; Nguyen, L.; Mehra, R. K. *J. Phys. Chem. A* **1999**, *103*, 10194.

NL0155274